

Electronic Supplementary Information

Morphology-controllable fabrication of organic microcrystals by solid-phase reactions: revealing morphology-sensitive highly efficient phosphorescence and enhanced near-infrared absorption

Guo-Ping Yong,* Chen Shen, Cong Zhang and Yu-Mei Zhao

Department of Chemistry, University of Science and Technology of China, Hefei 230026, P. R. China

E-mail: gpyong@ustc.edu.cn

Experimental procedures and measurements

Measurements

Microanalytical data (C, H, N) were collected on Vario ELIII elemental analyzer. FT-IR spectra were recorded using a Bruker EQUINOX55 FT-IR spectrophotometer. Mass spectrometry was carried out with Thermo Scientific Velos Pro mass spectrometer. The solution (10^{-5} M DMF) and solid-state UV/Vis/NIR absorption spectra were recorded at room temperature on a DUV-3700 UV/Vis/NIR spectrometer. The solid-state photoluminescence spectra and the decay lifetimes were determined at room temperature on a Fluorolog-3-TAU fluorescence spectrophotometer. The solid-state quantum yields were measured also on a Fluorolog-3-TAU fluorescence spectrophotometer equipped with a BaSO₄-coated integrating sphere. Powder X-ray diffraction (PXRD) patterns were collected on a Philips X'pert PRO SUPER diffractometer operating with nickel-filtered Cu-K α radiation ($\lambda = 1.540598 \text{ \AA}$) at 40 kV and 200 mA. Field-emission scanning electron microscopy (FE-SEM) measurements were performed with a FEI Sirion 200 field emission scanning electronic microanalyser operated at an accelerating voltage of 5 kV. The fluorescence microscopy images were obtained on an Olympus IX81 fluorescence microscope.

X-ray diffraction measurements were performed at 293(2) or 296(2) K on a Gemini S Ultra CCD diffractometer (Oxford diffraction Ltd.) using graphite monochromated Mo-K α ($\lambda = 0.71073 \text{ \AA}$). The structures were solved with the direct method and refined with a full-matrix least-squares technique with the SHELXTL program package. The empirical absorption correction (SCALE3 ABSPACK) was applied. All non-hydrogen atoms were refined with anisotropic displacement parameters. The C-H hydrogen atoms were generated geometrically and refined by the riding mode; the N-H hydrogen atom was located in the difference Fourier map and refined isotropically. Weighted R factor (R_w) and all goodness of fit S are based on F^2 , conventional R factor (R) is based on F .

Experimental procedures

All reagents were commercially available and used without further purification. 2,3'-Biimidazo[1,2-*a*]pyridin-2'-one radical (Hbipo^{•-}) was synthesized according to the previous procedure.^{S1}

Synthesis of BF₂-bipo complex (microcrystal **A**): 0.75 mL of BF₃·OEt₂ (6.00 mmol) was slowly injected into 30 mL of DMF containing 1.00 g (4.00 mmol) of Hbipo^{•-}. The reaction system was stirred at 80 °C for 1 day, resultant solid was collected by filtration and washed with DMF and water, and then dried in air at 75°C for 8 h, affording pale yellow microcrystal **A** (68.75% Yield). HRMS (EI, m/z, [M]⁺): calcd for C₁₄H₉BF₂N₄O: 298.06; found: 298.17. Anal. calcd for C₁₄H₉BF₂N₄O: C 56.42, H 3.04, N 18.80; found: C 56.16, H 3.12, N 18.55. The microcrystal **A** was added to DMSO, and heated at 80 °C till solid was completely dissolved. Yellow single crystal **A** was obtained by slowly decreasing temperature (from 80 °C to room temperature).

Fabrication of BF₂-HbipoCl (Microcrystal **B** or **C**): At room temperature, 1.49 g (5.00 mmol) of BF₂-bipo was dissolved in 40 mL of CH₃CN-HCl solution (CH₃CN:HCl (36 %) = 1:1, v/v), and made to stand at room temperature for 1 week, the white microcrystal **B** (BF₂-HbipoCl) was obtained, which then was collected by filtration and dried in air at 75°C for 8 h (73.00% Yield). Anal. calcd for C₁₄H₁₀BClF₂N₄O: C 50.27, H 3.01, N 16.75; found: C 49.92, H 3.08, N 16.80. The white microcrystal **C** can be fabricated by exposure BF₂-bipo to HCl vapor in a closed container within 30 min.

Fabrication of BF₂-HbipoClO₄ (Microcrystal **D**): At room temperature, 1.34 g (4.00 mmol) of microcrystal **B** or **C** was immersed to 40 mL H₂O. To this stirred system, 0.40 mL (5.00 mmol) of 70 % HClO₄ aqueous solution was dropwise added. The resulting solid-phase anion exchange reaction system was stirred at room temperature for 30 min, then filtered off and dried in air at 75°C for 8 h (93.50% Yield). Anal. calcd for C₁₄H₁₀BClF₂N₄O₅: C 42.19, H 2.53, N 14.06; found: C 41.85, H 2.67, N 14.15. Colorless columnar single crystal **D** was obtained by slow volatilization of CH₃CN solution of microcrystal **D** at room temperature.

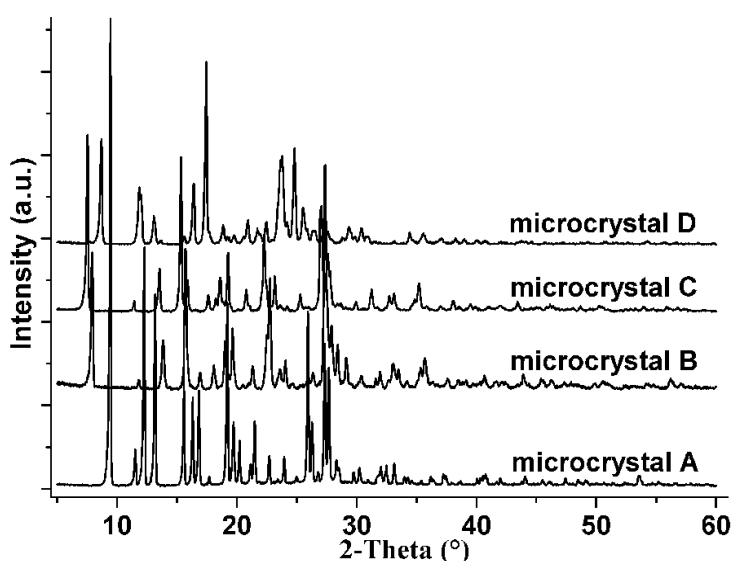


Fig. S1 PXRD patterns of microcrystals **A**, **B**, **C** and **D**.

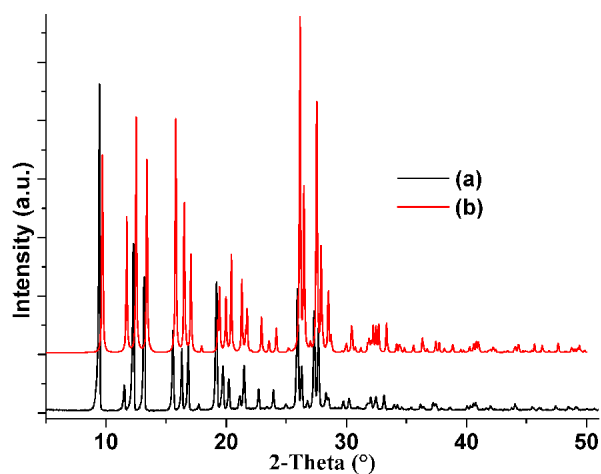


Fig. S2 The PXRD pattern of microcrystal **A** (a) and calculated PXRD pattern by using the Mercury program based on the single crystal X-ray diffraction data of single crystal **A** (b).

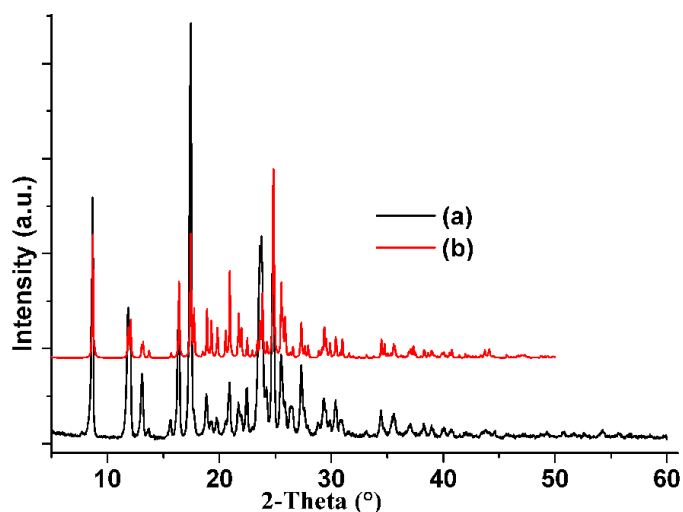


Fig. S3 The PXRD pattern of microcrystal **D** (a) and calculated PXRD pattern by using the Mercury program based on the single crystal X-ray diffraction data of single crystal **D** (b).

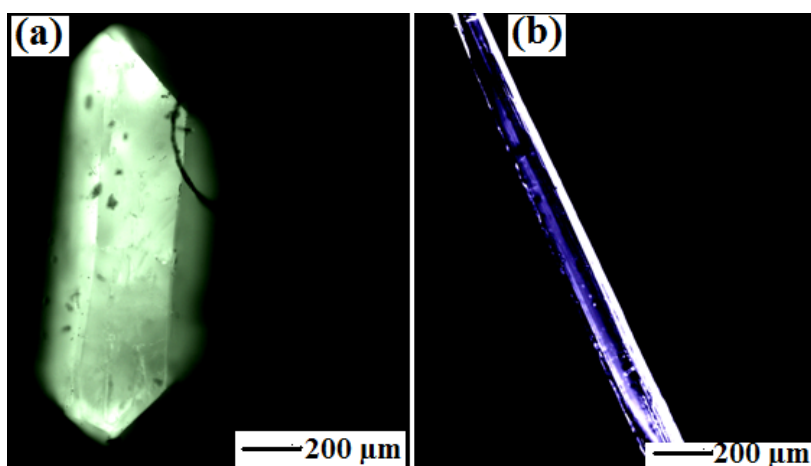


Fig. S4 Fluorescence microscopy images of single crystals **A** (a) and **D** (b).

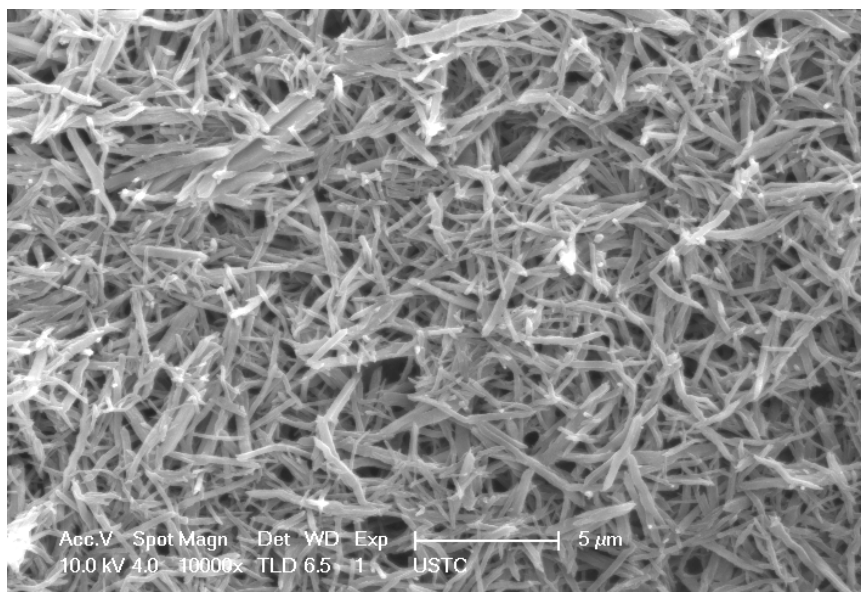


Fig. S5 SEM image of 1D microrods of microcrystal **D** prepared from $\text{CH}_3\text{CN-HClO}_4$ solution.

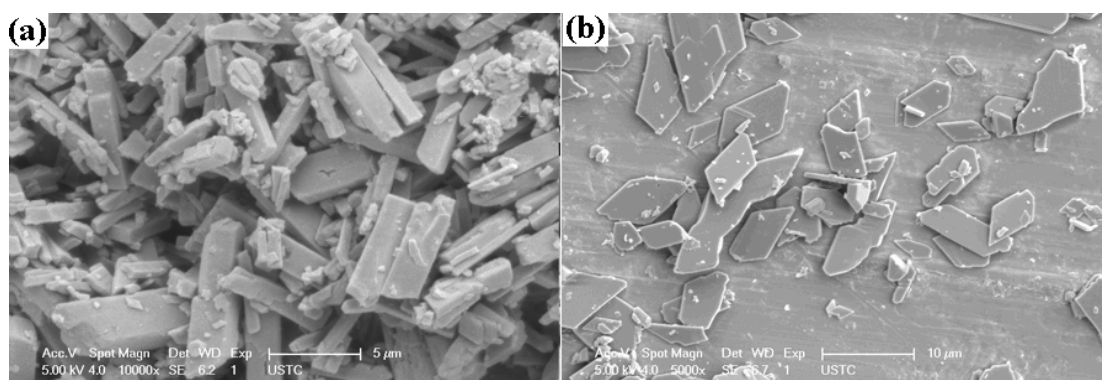


Fig. S6 SEM images of 3D microbricks (a) and 2D rhombic microsheets (b) prepared by immersing $\text{BF}_2\text{-HbipoCl}$ to 15 % HNO_3 and 8 % KPF_6 aqueous solution at room temperature, respectively. The results indicate that the solid-phase anion exchange induced morphological change from 2D hexangular microflakes to 3D microbricks or 2D rhombic microsheets is remarkable, further supporting that the anions really play an important role in controlling morphologies.

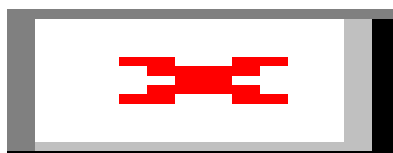


Fig. S7 ORTEP drawings with atom labeling of complexes $\text{BF}_2\text{-bipo}$ (a) and $\text{BF}_2\text{-HbipoClO}_4$ (b) with 50% probability ellipsoids.

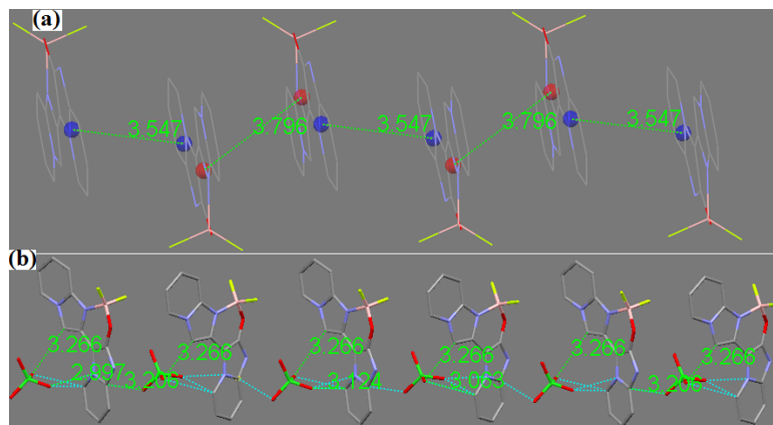


Fig. S8 The 1D chain structure of BF₂-bipo (a) assembled by π - π stacking interactions, and BF₂-HbipoClO₄ (b) assembled by short atomic contacts and anion- π interactions.

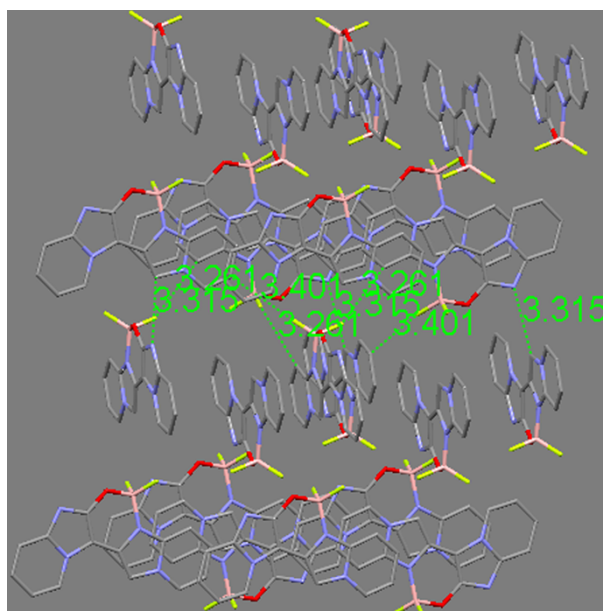


Fig. S9 The 2D layer of BF₂-bipo crystal assembled by short atomic contacts.

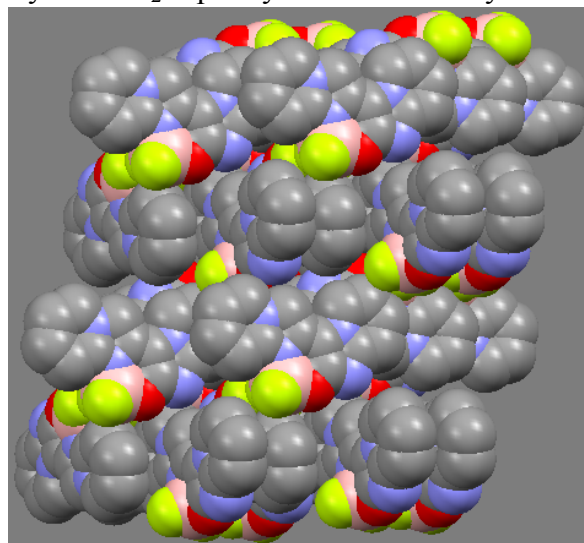


Fig. S10 Space-filling diagram represents the 3D structure of BF₂-bipo crystal.

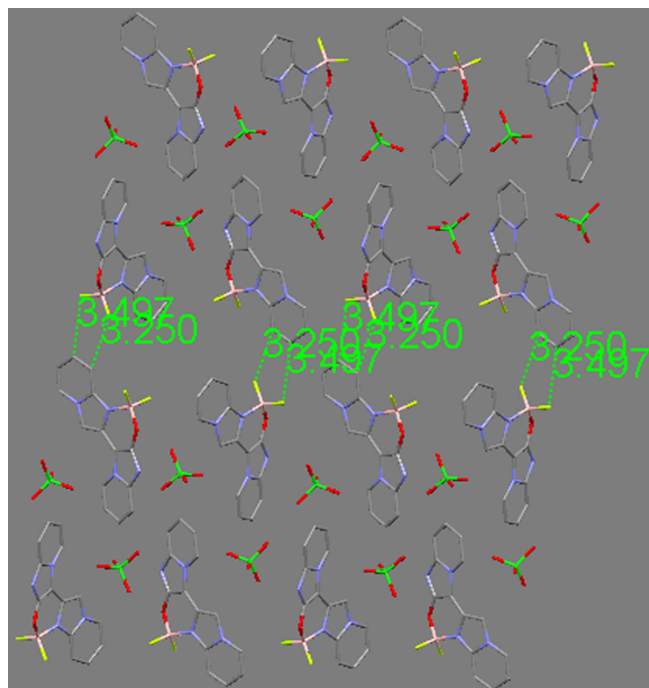


Fig. S11 The 2D layer of $\text{BF}_2\text{-HbipoClO}_4$ crystal assembled by short atomic contacts.

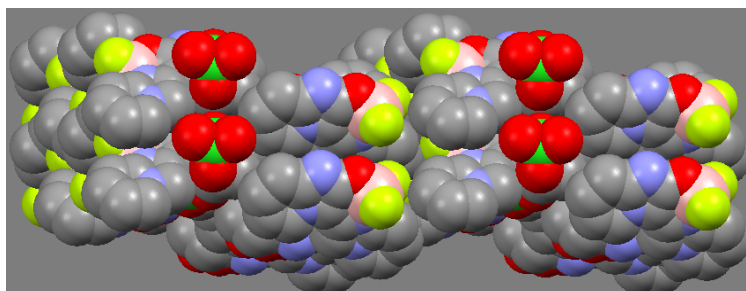


Fig. S12 Space-filling diagram represents the 3D structure of $\text{BF}_2\text{-HbipoClO}_4$ crystal.

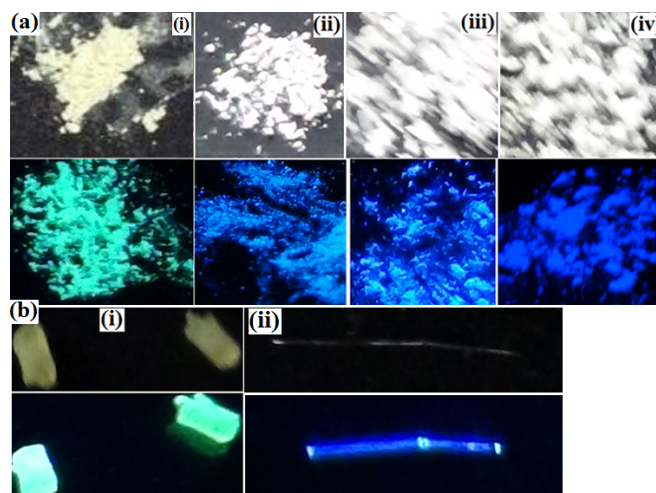


Fig. S13 (a) Photographs of microcrystals **A** (i), **B** (ii), **C** (iii) and **D** (iv) under a 365 nm UV lamp irradiation (below) and under ambient light (up); (b) Photographs of single crystals **A** (i) and **D** (ii) under a 365 nm UV lamp (below) and ambient light (up).

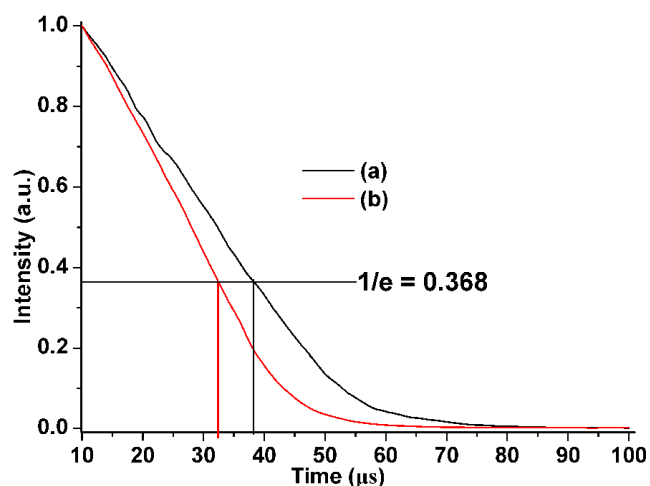


Fig. S14 The decay lifetime curves of microcrystals **A** (a) and **B** (b) at emission peak of 514 and 455 nm, respectively in solid state. The lifetime (τ) is defined as the time in which the emission intensity decays to $1/e$ of the initial intensity (I_0), where e is the natural log constant and is equal to 2.718. ($I = I_0 e^{-(t/\tau)} \Rightarrow \tau = t \Rightarrow I = (1/e) I_0$).^{S2}

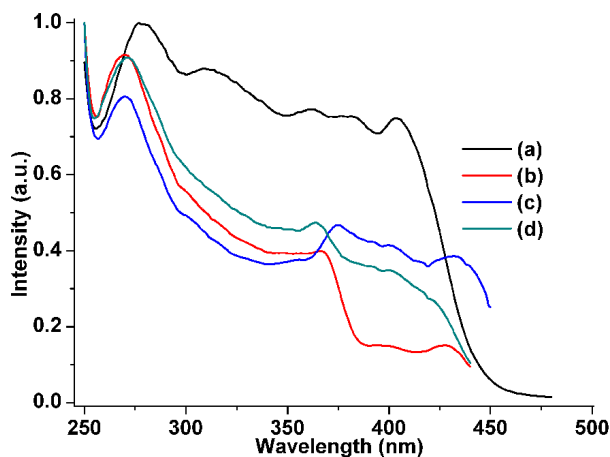


Fig. S15 Room-temperature solid-state excitation spectra of microcrystallines **A** (a), **B** (b), **C** (c) and **D** (d).

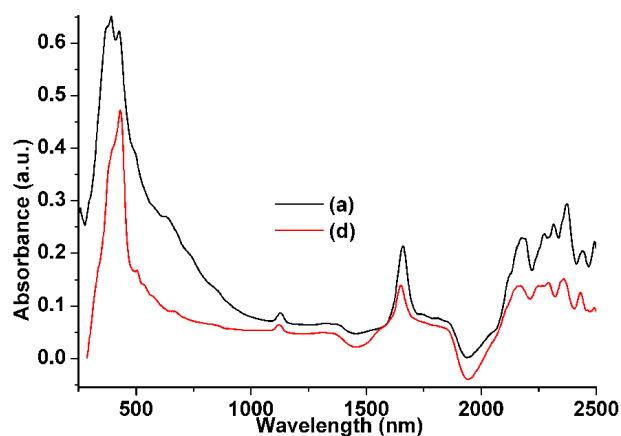


Fig. S16 UV/Vis/NIR absorption spectra of microcrystals **A** (a) and **D** (d) in solid state.

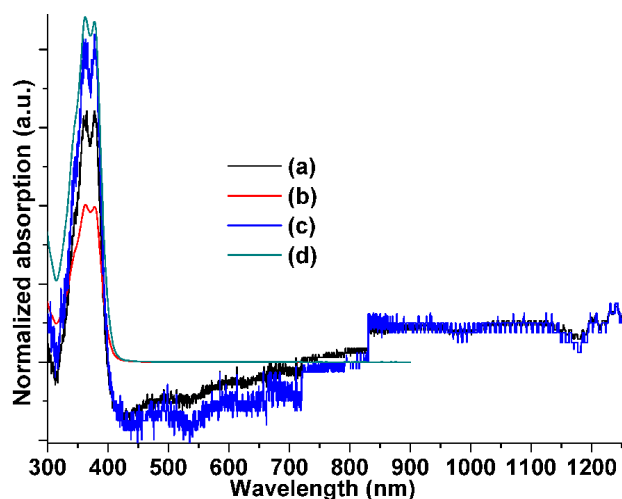


Fig. S17 Normalized UV/Vis/NIR absorption spectra of microcrystals **A** (a), **B** (b), **C** (c) and **D** (d) in 10^{-5} M DMF solution.

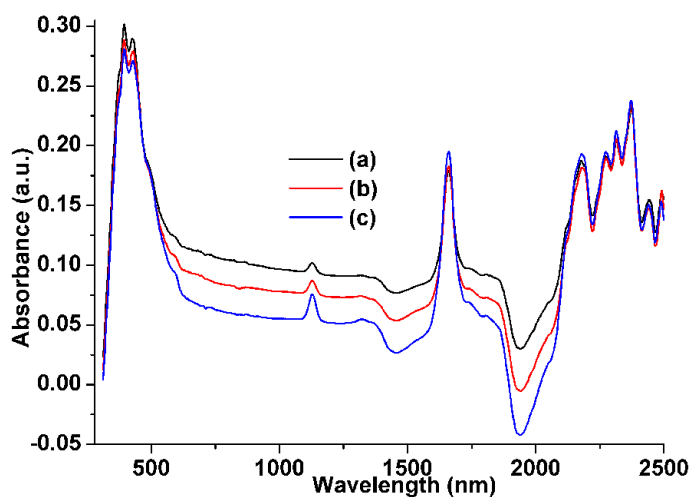


Fig. S18 UV/Vis/NIR absorption spectra of microcrystal **A** with the solid dosage of 50 mg (a), 100 mg (b) and 150 mg (c), respectively.

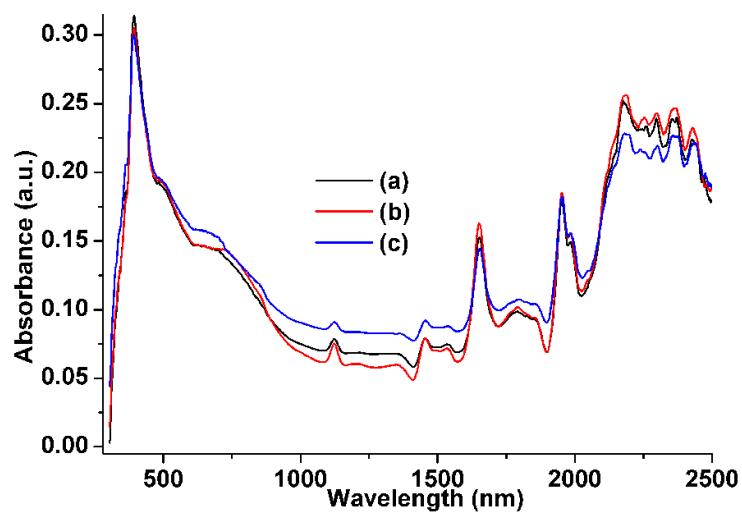


Fig. S19 UV/Vis/NIR absorption spectra of microcrystal **B** with the solid dosage of 50 mg (a), 100 mg (b) and 150 mg (c), respectively.

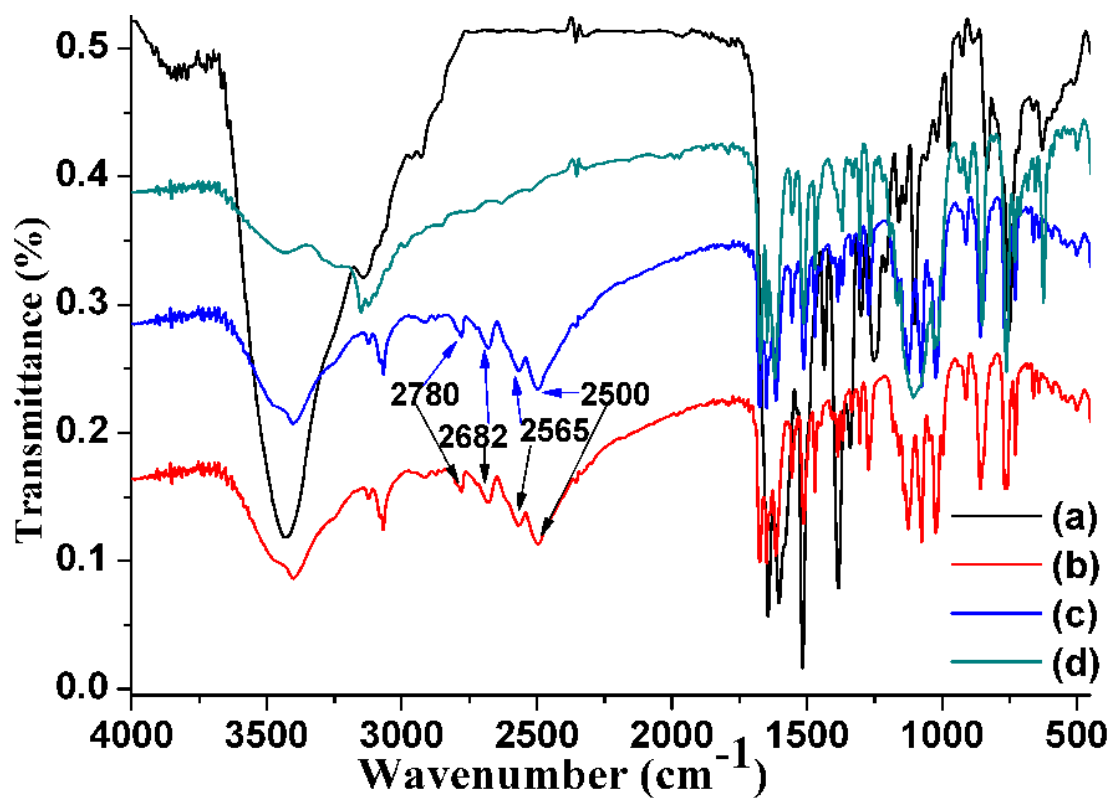


Fig. S20 FT-IR spectra of microcrystals A (a), B (b), C (c) and D (d).

Reference

S1 G. P. Yong, C. F. Li, Y. Z. Li and S. W. Luo, *Chem. Commun.*, 2010, **46**, 3194.

S2 K. C. Stylianou, R. Heck, S.Y. Chong, J. Bacsá, J. T. A. Jones, Y. Z. Khimyak, D. Bradshaw and M. J. Rosseinsky, *J. Am. Chem. Soc.*, 2010, **132**, 4119.